



External Geophysics, Climate and Environment

The impact of Cyclone Nargis on the Ayeyarwady (Irrawaddy) River delta shoreline and nearshore zone (Myanmar): Towards degraded delta resilience?

Manon Besset^{a,*}, Edward J. Anthony^a, Philippe Dussouillez^a, Marc Goichot^b^a Aix-Marseille University, CNRS, IRD, CEREGE UM34, 13545 Aix-en-Provence, France^b Lead, Water and Energy Security, WWF Greater Mekong, 18, Tu Xuong street, Ward 7, District 3, Ho Chi Minh City, Viet Nam

ARTICLE INFO

Article history:

Received 11 May 2017

Accepted after revision 22 September 2017

Handled by Isabelle Manighetti,
Rutger De Wit, Stéphanie Duvail,
and Patrick Seyler

Keywords:

Ayeyarwady River delta
Cyclone Nargis
Delta shoreline erosion
Delta resilience
D Brielta vulnerability

ABSTRACT

The Ayeyarwady River delta (Myanmar) is exposed to tropical cyclones, of which the most devastating has been cyclone Nargis (2–4 May 2008). We analysed waves, flooded area, nearshore suspended sediments, and shoreline change from satellite images. Suspended sediment concentrations up to 40% above average during the cyclone may reflect fluvial mud supply following heavy rainfall and wave reworking of shoreface mud. Massive recession of the high-water line resulted from backshore flooding by cyclone surge. The shoreline showed a mean retreat of 47 m following Nargis. Erosion was stronger afterwards (−148 m between August 2008 and April 2010), largely exceeding rates prior to Nargis (2000–2005: −2.14 m/year) and over 41 years (1974–2015: −0.62 m/year). This implies that resilience was weak following cyclone impact. Consequently, the increasingly more populous Ayeyarwady delta, rendered more and more vulnerable by decreasing fluvial sediment supply, could, potentially, become more severely impacted by future high-energy events.

© 2017 Académie des sciences. Published by Elsevier Masson SAS. This is an open access article under the CC BY-NC-ND license (<http://creativecommons.org/licenses/by-nc-nd/4.0/>).

1. Introduction

River deltas are commonly highly productive environments that offer rich and biodiverse ecosystems and a wide range of ecosystem services, such as coastal defence, drinking water supply, recreation, green tourism, and nature conservation. Deltas are characterized, however, by low topography, and are, thus, particularly vulnerable to catastrophic river floods, tsunamis, and cyclones. Deltas may develop morpho-sedimentary resilience to these high-energy events. This commonly occurs through reorganization of delta morphology, notably channel patterns, and changes in sedimentation (Anthony, 2016).

However, human impacts, coupled with the effects of climate change, are rendering many deltas economically and environmentally vulnerable, resulting in weakening of their resilience (Brondizio et al., 2016; Ericson et al., 2006; Syvitski et al., 2009). This vulnerability is increasing because of reduced sediment flux from rivers and various other modifications caused by human interventions. A better understanding of delta dynamics and vulnerability is needed in order to implement viable delta restoration and rehabilitation strategies.

Myanmar is the largest country in Southeast Asia, with an area of 676,600 km², and the country relies heavily on the economic advantages provided by the Ayeyarwady (Irrawaddy) River basin and its delta (Fig. 1). As in most developing countries, population growth has been extremely rapid, increasing the risk potential associated with river flooding, storm surge activity, and coastal erosion.

* Corresponding author.

E-mail address: besset@cerge.fr (M. Besset).

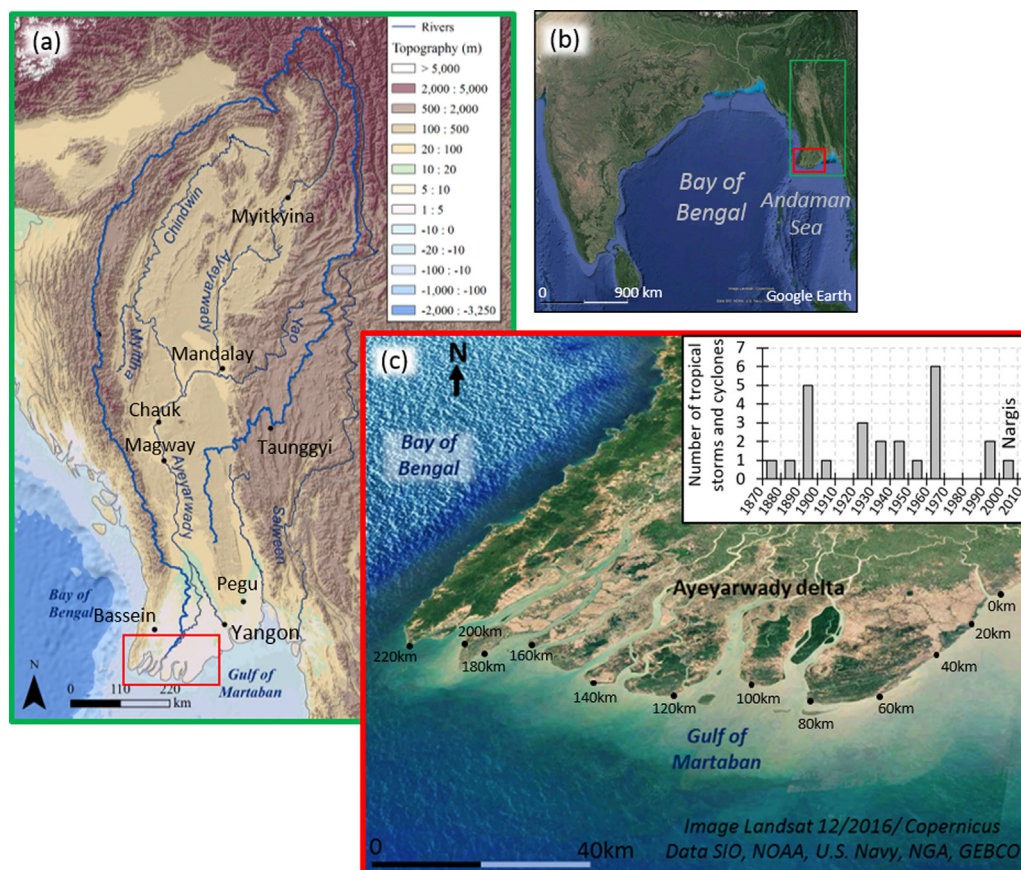


Fig. 1. Shaded-relief map showing physical features of Myanmar and the Ayeyarwady River basin (a, b), and Google Earth image of the Ayeyarwady delta (c) with indications of alongshore kilometric points (from east to west) used to identify shoreline sectors. The inset in (c) shows tropical storms and cyclones over the Ayeyarwady River delta from 1870 to present.

Data from International Best Track Archive for Climate Stewardship (IBTrACS), Knapp et al. (2010).

About 15 million, out of Myanmar's current population of 51.4 million, reside in the Ayeyarwady delta, according to the provisional results of the 2014 census (official estimates of nearly 60 million), and this represents an increase by nearly 150% in about 30 years (Brakenridge et al., 2017). The delta offers large areas of rich agricultural land and is one of the most productive rice-growing areas in the world. About 60% of the delta is currently under rice cultivation (Frenken, 2012).

Myanmar is, however, among the 15 nations that together account for 80% of the world's population exposed to river flood risk (Ward et al., 2013; Winsemius et al., 2013). This risk is particularly pertinent to the vast Ayeyarwady delta (Brakenridge et al., 2017), the world's tenth largest delta (Coleman and Huh, 2004). The Bay of Bengal is affected by tropical cyclones and Myanmar lies in the pathway of these high-energy events, over 25 of which have affected the Ayeyarwady delta (Fig. 1c) since 1870 (Knapp et al., 2010). Tropical cyclonic storms make landfall in Myanmar between May and October, and generate heavy rainfall and severe flooding (Brakenridge et al., 2017). Tropical Cyclone Nargis (2–4 May 2008), a category-5 event just prior to landfall in Myanmar, is the latest and strongest meteorological event to have affected the delta in

historic times (Fritz et al., 2009), the other recorded events being mainly of categories 1 to 2 (Fig. 1c). These high-energy events may also cause storm surges that further aggravate coastal flooding and damage (Dube et al., 2010). Prior to Nargis, the 10 May 1968 cyclone gives a measure of the deadly damage susceptible to be caused by cyclones in Myanmar (Brakenridge et al., 2017). This cyclone killed 1037 people, left 17,537 livestock dead, close to 300,000 people homeless, and 57,663 homes destroyed (USAID, 1968).

Tropical cyclone Nargis caused the worst natural disaster in the recorded history of Myanmar (Fritz et al., 2009; Topich and Leitich, 2013; Wolf, 2009). According to these authors, fatality estimates exceeded 138,000, at least 2.4 million people were severely affected and over a million people were left homeless. An estimated 90–95% of the buildings in the delta, and much farmland, livestock, and fisheries were lost, and the overall economic damage estimated at over 10 billion US\$ (Fritz et al., 2009). These extreme casualties and damages resulted from a cyclone surge that ranged from 1.9 to 5.6 m, and that led to flooding up to 50 km inland (Fritz et al., 2009). Using satellite images, Brakenridge et al. (2017) mapped the vast land areas affected by the Nargis coastal storm surge and

unusual inland rainfall. Major flooding was restricted to the delta and lower floodplain areas.

In this paper, we address the issue of the effects of this high-energy event on shoreline stability and on coastal and nearshore sedimentation. We then discuss these effects in the context of the current vulnerability of the Ayeyarwady delta, increasingly subject to the impacts of human activities in both the river catchment and delta, and considered as a delta 'in peril' by [Syvitski et al. \(2009\)](#).

2. The Ayeyarwady River basin and delta

The Ayeyarwady River ([Fig. 1b](#)) has the second largest watershed in Southeast Asia, after the Mekong. The river covers slightly over 61% of the territory of Myanmar, and its delta ([Fig. 1c](#)) has formed 20,570 km² of low, fertile plain comprising five major and many smaller distributaries ([Brakenridge et al., 2017](#)). The Ayeyarwady basin's climate is tropical monsoon. Rainfall is concentrated in the hot humid months of the southwest monsoon (May–October), as the Inter-Tropical Convergence Zone (ITCZ) attains its most-northward position between June and August, and humidity-charged southwest winds blow northeastwards across the Bay of Bengal. In contrast, the northwest monsoon (December–March), characterized by opposite dry northwest winds blowing southeast from the continent, is relatively cool and almost entirely dry. The mean annual rainfall across the delta ranges from 2000 to 3000 mm ([Frenken, 2012](#)). Another source of water for the rivers is summer melting of the snow and glaciers in mountainous northern Myanmar, which also contributes to flow variability. Heavy rains in the mountains, coupled with snowmelt, generate large flood volumes, and this water can cause large-scale downstream overbank flooding ([Brakenridge et al., 2017](#)).

According to [Van der Velden \(2015\)](#), the combined discharge of the Ayeyarwady and Chindwin Rivers at Chauk ([Fig. 1](#)) ranges widely from 1500 m³/s to about 30,000 m³/s; or at the head of the delta from about 2000 m³/s to about 33,000 m³/s. [Robinson et al. \(2007\)](#) calculated an Ayeyarwady delivery of 44,241 km³ of water, containing 226–364 Mt of sediment, to the ocean every year, much of this supply being seasonally. The data compiled by [Robinson et al. \(2007\)](#) and collected between 1969 and 1996 at Pyay (Prome) were further analysed by [Furuichi et al. \(2009\)](#) to provide an estimate of water discharge ($379 \pm 47 \cdot 10^9$ m³/year) and suspended sediment load ($325 \pm 57 \cdot 10^6$ t/year) for the river upstream of the delta head. In the face of these values of water discharge and suspended sediment load, the water turbidity will be approximately 600 g/m³ at the mouths of the Ayeyarwady ([Kravtsova et al., 2009](#)), which corresponds to relatively high values.

The Ayeyarwady delta is affected by waves of moderate fetch (wave periods of 8–12 s with a mean of about 10 s) generated by the southwesterly winds, and thus, almost exclusively from a southwesterly direction. Wave heights are characterized by marked seasonal variability ([Anthony et al., 2017](#)). They are highest (mean values of up to 2 m) at the peak of the rainy southwest monsoon season, and diminish during the dry season when the southwest

monsoon winds become attenuated due to the southward migration of the ITCZ. Maximum wave heights can reach 5 m during cyclones. Longshore currents generated by southwest monsoon winds and waves are, together with tidal currents, important in transporting both bedload material (sand) along the beaches bordering the delta, and suspended sediment, which dominates the load of the Ayeyarwady. Longshore currents flow dominantly from west to east in response to the dominant wave approach from the southwest. Reversals of these currents are locally observed, especially near the mouths of the larger delta distributaries where wave refraction commonly leads to bi-directional currents with beach sand transport materialized by spits.

The Ayeyarwady delta is associated with relatively large semidiurnal tides ranging from 3 to 6 m. Data collated by [Kravtsova et al. \(2009\)](#) show that the mean tidal range is 3.0 m in the western part of the delta shoreline and about 3.2 m in the east. Mean spring and neap tidal ranges along the western extremity of the delta are 4 m ([Ramaswamy et al., 2004](#)) and 1.8 m ([Kravtsova et al., 2009](#)), respectively, but up to 5.85 m and 2.55 m ([Naing, 2014](#)), respectively, along the eastern shores of the delta. Spring tide influence extends almost 300 km inland to the apex of the delta ([Hedley et al., 2010](#)).

The protruding western part of the delta, comprising numerous lobes separated by distributary mouths ([Fig. 1c](#)), has prograded much more than the more sheltered eastern half. The exposed western shores are characterized by 20–100-m-wide sandy beaches bounding muddy backshore swales hundreds of meters in width, essentially devoted to rice cultivation. The beaches are commonly subject to overwash and landward migration in a context of chronic erosion ([Anthony et al., 2017](#); [Hedley et al., 2010](#)), and are fronted by muddy foreshores hundreds of meters wide at low tide, commonly exhibiting signs of erosion ([Fig. 2](#)). The succession of narrow beach ridges and broad intervening swales characterizing the 2–3-km-wide coastal fringe of the Ayeyarwady delta in the western sector appears to represent the mode of deltaic progradation in this sector, whereas the more sheltered, but less prograded, eastern sector has been characterized by dominantly muddy sedimentation associated with mangrove colonization.

Since 1974, a year marking the advent of the availability of satellite images, erosion has affected about 240 km of the 450-km-long delta shoreline, i.e. 53%, essentially in the western sector ([Anthony et al., 2017](#)), where are located, paradoxically, the delta's main distributors of fluvial sediment to the coast. According to [Rodolfo \(1969\)](#), the Ayeyarwady delta prograded at an average rate of 2.5 km in 100 years into the Andaman Sea up to the start of the last quarter of the 20th century. The current dominant shoreline erosion pattern thus represents a major turnaround from generalized progradation ([Anthony et al., 2017](#)), a conclusion in agreement with [Hedley et al. \(2010\)](#), who identified a long phase of equilibrium prior to 1989, during which sediment deposition balanced subsidence and sea level rise, followed by net erosion from 1989 to 2006. [Hedley et al. \(2010\)](#) further predicted more shoreline erosion in the coming years because of projected dam constructions in the Ayeyarwady catchment.



Fig. 2. Ground photographs (November 2016) of the sandy beaches and large, muddy low tide foreshore fringing the western sector of the Ayeyarwady

3. Methodology

To monitor the effects of cyclone Nargis on the Ayeyarwady delta, we:

- collated information on the cyclone track;
- collected offshore wave and tidal data;
- downloaded data on surface-suspended particulate matter (SPM) concentrations offshore of the delta;
- mapped flooding of the coastal fringe and changes in the position of the high-water line alongshore.

The cyclone track was determined from the UNOSAT cyclone database. Offshore wave data covering the landfall of the cyclone (2–4 May, 2008) were analysed from the ERA-Interim hindcast wave database generated by the European Centre for Medium-Range Weather Forecasting (ECMWF) Wave Atmospheric Model. Mean wave directions ($^{\circ}$), significant wave heights (m), and periods (s) were obtained for the period 27 April to 1 June 2008. The astronomical tides off the delta for the period 1–8 May

2008 were downloaded from the tide and current prediction programme WXTide32[®] for Yangon.

Two MODIS satellite images (NASA/MODIS Rapid Response Team) of the coastal fringes were consulted to show the state of flooding of the delta prior to 15 April 2008 and following the landfall of cyclone Nargis (5 May 2008). Changes in the high-water line alongshore, prior to and following Nargis, were digitized from a total of eight LANDSAT satellite images (30 m pixel size) covering three dates (18 April, 4 May, and 24 August 2008, Fig. SM1), which correspond to the dates of the best available satellite images in terms of cloud cover and comparable tidal range. The 4 May image provided a record of the position of the high-water line just after the cyclone landfall. These three dates therefore represent, respectively, the pre-cyclone, the cyclone landfall, and the post-cyclone high-water line coverage. In order to assess the state of the delta shoreline over a year and a half after Nargis, a fourth set of satellite images (25 April 2010) was analysed. For all images, other than those of 4 May, a variety of indicators, notably farm houses and the landward limits of dry sandy beaches in the

western sector, and the mangrove fringe in muddy areas where beaches are missing, were used to delimit the high-water line. The use of these types of marker was not feasible for the 4 May image, which coincided with strong water level setup caused by the significant cyclone-induced surge (Fritz et al., 2009). For this date, we resorted to the visible brush, plantation or mangrove fringe. Changes in the high-water line along 250 km, out of the 450 km, of delta shoreline, were calculated using the ArcMap extension module Digital Shoreline Analysis System (DSAS), version 4.3, coupled with ArcGIS® 10.2.2. Determination of change rates focused on the exposed western sector of the delta, which took the brunt of the cyclone (see “Results” section), and where surge levels were highest (Fritz et al., 2009). We setup a transect every 100 m alongshore from which variations between the changing high-water (or vegetation for the 4 May image) line and a pre-determined inland base line were calculated between the successive sets of LANDSAT images. This distance was calculated between two image dates to generate statistics of shoreline change in DSAS 4.3. We retained a relatively large uncertainty shoreline change band of ± 42 m, which is much more than commonly used in the literature. We defined the error (E) of shoreline change from the following equation (Hapke et al., 2006):

$$E = \sqrt{(d_1^2 + d_2^2)}$$

where d_1 and d_2 are the uncertainty estimates, respectively of resolution and georeferencing, for the successive sets of images.

Finally, recently collated MERIS satellite data on suspended particulate matter (SPM) offshore of the Ayeyarwady delta (GlobCoast project, <http://sextant.ifremer.fr/en/geoportail/sextant>) were used to determine the impact of cyclone Nargis on nearshore fine-grained sediment spread in 2008 by comparing monthly values prior to, during, and after Nargis with averages over a 10-year period (2002–2012).

4. Results

The track of cyclone Nargis is shown in Fig. 3a. The cyclone attained category 5 just prior to landfall in Myanmar, moved ashore as a category-4 event, gradually weakened after passing Yangon with winds of 215 km/h on 2 May, and dissipated near the border between Myanmar and Thailand. The shores and multiple mouths in the protruding western half of the delta thus took the brunt of the cyclone, whereas the embayed muddy mangrove-colonized eastern sector in the Gulf of Martaban was relatively less exposed because of a more inland cyclone trajectory and weaker winds (Fig. 3a). Fig. 3b and c show, respectively, an extract of ERA-Interim offshore wave conditions (red rectangle) and tides during the course of the cyclone. Relatively high waves of up to 3 m, associated with wind-wave periods of 7 to 9 s and directions that were essentially from southwest, occurred briefly on 3 May, just after the cyclone made landfall in a frontal approach relative to the delta shoreline in the western sector. Waves prior to, and following this relatively brief phase, did not exceed 2 m, and were hardly higher than 1 m

by 5 May. Landfall, just after 2 May, was characterized by a transition from neap to spring tides. Spring tides were attained on 5 May (Fig. 3c).

Two MODIS images in Fig. 4 show the extent of catastrophic flooding of the delta on 5 May 2008, compared to the pre-cyclone state of the delta on 15 April 2008. The figure also shows maps, established by Brakenridge et al. (2017), indicating the strong rainfall that accompanied Nargis. The high-water line used as a proxy for the shoreline showed a mean retreat of 47 m on 24 August 2008, three months after the cyclone, compared to the 18 April high-water line. Retreat locally exceeded 200 m along the exposed western part of the delta, whereas the transitional zone towards the embayed eastern sector showed little change, notably between km 0 and km 10 (Fig. 5a). The data of 25 April 2010 showed even more significant landward translation (average: -148 m) of the high-water line 20 months after the passage of Nargis (Fig. 5b). In order to determine to which extent flooding of the coast occurred in response to the increase in sea level caused jointly by the cyclone surge, the large waves and the spring tide range (Fig. 3), the 18 April and 4 May high-water lines were compared (Fig. 6), the latter representing the situation barely 36 h after the cyclone landfall on 2 May 2008. The results show a landward translation of the high-water line that attained 600 m in places.

The offshore concentrations in SPM in 2008 show a significant increase during the passage of Nargis, compared to the monthly averages based on the 10-year SPM dataset (Fig. 7a). From January to April, the monthly values followed fairly closely the 10-year average trend. In contrast, increasing SPM values occurred in May, specifically during the passage of Nargis, with an average concentration increase of nearly 50% ($\pm 5\%$) over the region of the delta compared to April (Fig. 7b, c), and representing a 38% increase relative to the 10-year average over the same period. In the area directly affected by the intensity peak of the cyclone, the increase attained about 100% (Fig. 7c), which is 70% higher than the 10-year average. The values diminish once again in the two months following Nargis (May–June, Fig. 7d, and June–July, Fig. 7e) to attain the 10-year average, before increasing once again as the rainy season gained momentum in July–August (Fig. 7f).

5. Discussion

Large modern river deltas represent huge coastal sediment storage, and thus, generally, show morpho-sedimentary resilience in the wake of high-energy events. A consideration of the wave heights, tidal range (Fig. 3b, c), and the storm surge levels (1.9–5.6 m) determined by Fritz et al. (2009) in their post-Nargis field survey in August 2008, three months after the cyclone, suggests that the high-water line determined from the 4 May 2008 image (Fig. 6) is a good proxy highlighting the extent of backshore flooding caused by Nargis. Once the narrow beaches were flooded, the high-water line shifted landwards, up to hundreds of metres in places (Fig. 6), as the large low backshore swales were submerged in turn. The extent of flooding is depicted by comparison of the MODIS images in Fig. 4. Nargis flooded about 14,400 km² of the delta

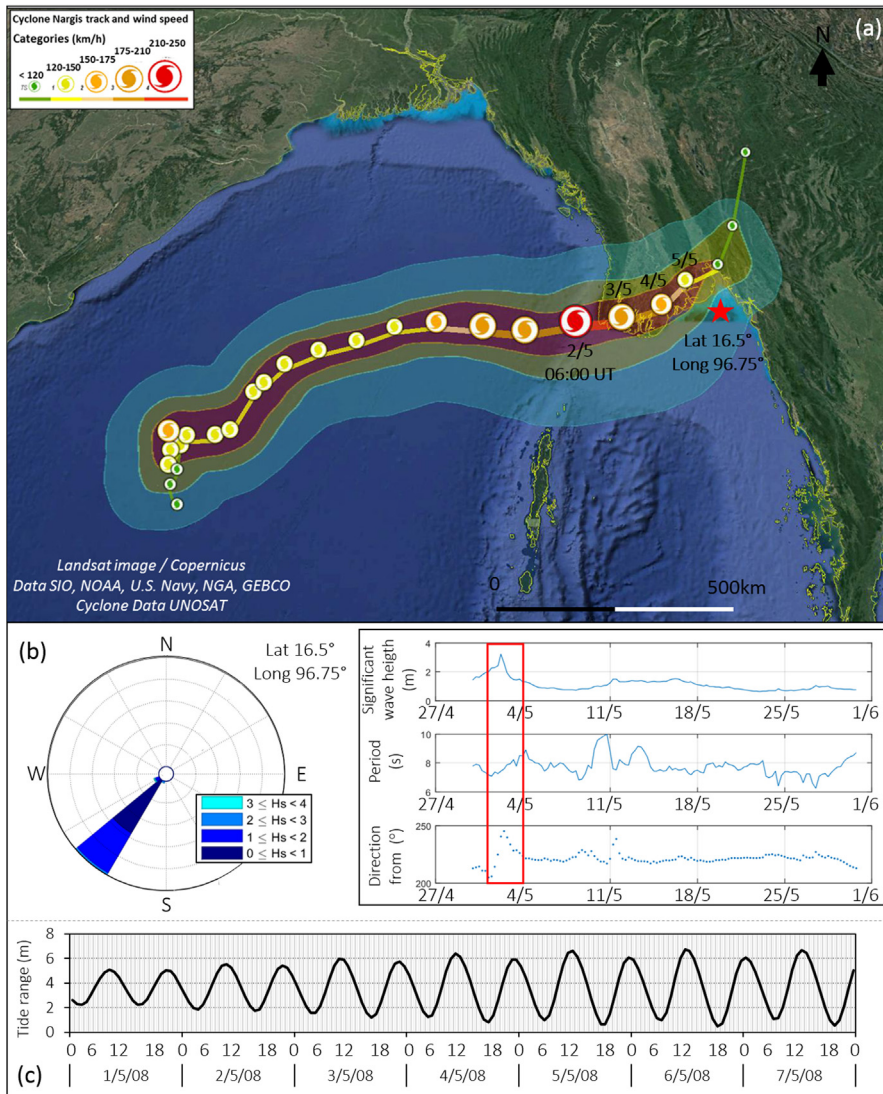


Fig. 3. Trajectory of Tropical Cyclone Nargis in May 2008 on a 6-h-time lapse from 18 April 2008 (12:00 UT) to 4 May 2008 (00:00 UT) from the UNOSAT Cyclone data base (a), wave climate offshore of the Ayeyarwady delta during the passage of Nargis (red rectangle) computed from the ERA-Interim hindcast wave database generated by the European Centre for Medium-Range Weather Forecasting (ECMWF) Wave Atmospheric Model (b), and astronomical tides off the delta (c) from the tide and current prediction programme *WXTide32*® (Version 4.6). Nargis' direction of approach from the west resulted in maximum winds having a counterclockwise circulation in the shallow offshore area, and the protruding western sector of the delta took the brunt of the cyclone. Fritz et al. (2009) reported a storm surge ranging from 1.9 to 5.6 m above sea level along this western sector.

inland (Tasnim et al., 2015). Although high waves associated with the cyclone lasted only about 12 h, and peak wave heights only briefly attained 3.2 m, the marked shoreline retreat between April and August 2008 (Fig. 5a) highlights the significant impact of Nargis on the narrow sandy beaches and their large muddy foreshores. These retreat rates are similar to those reported by Fritz et al. (2009) following their field survey in the delta, in the course of which they identified erosion of up to 150 m in places. As these authors noted, these rates are also similar to those generated by Hurricane Katrina impacting on the Mississippi delta barrier islands in 2005, with surge levels ranging from 2 to over 10 m (Fritz et al., 2007). Between 2004 and 2005, hurricane Katrina resulted in a landward

retreat of 201.5 m of the northern shorelines of the low-lying Chandeleur islands, compared to an average retreat rate of 38.4 m between 1922 and 2004 (Fearnley et al., 2009). The impact of Nargis on the Ayeyarwady delta shoreline thus provides another very good example of the effects of a severe cyclone on low deltaic shorelines, especially where a longer-term background context of erosion prevails, which is also the case of parts of the Mississippi delta.

The marked and persistent erosion 20 months after Nargis (Fig. 5b) shows the absence of resilience along much of the affected delta shoreline, and is consistent with the state of chronic shoreline erosion affecting this delta (Anthony et al., 2017; Hedley et al., 2010) at least since

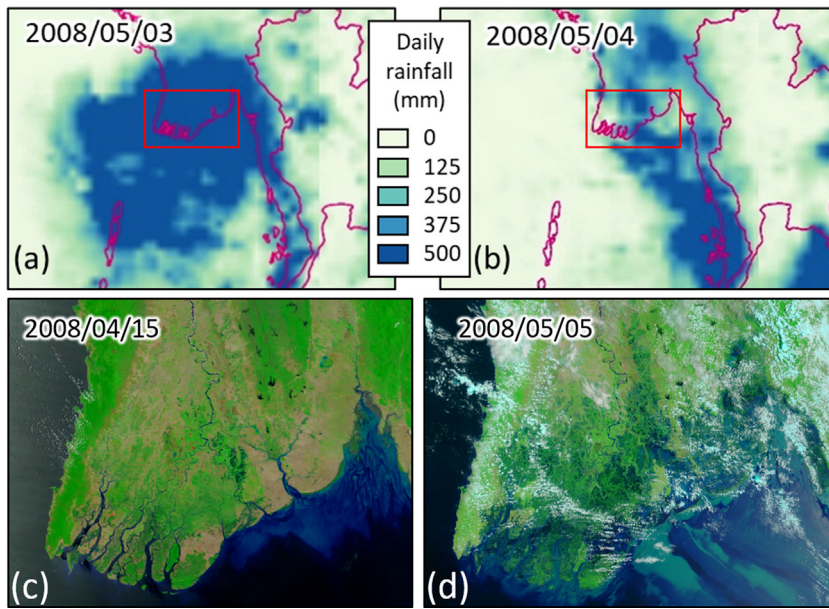


Fig. 4. Rainfall and flooding in the Ayeyarwady delta generated by Cyclone Nargis: (a) maps showing annual maximum monsoon inundation levels for 2013 and 2014 (light blue), and rainfall on 3 May (a) and 4 May 2008 (b) in the western Bay of Bengal (from [Brakenridge et al., 2017](#), with permission from Elsevier); (c, d) MODIS satellite images showing the delta prior to cyclone Nargis on 15 April 2008, and the devastating flooding on 5 May 2008 (following the cyclone's landfall in the Ayeyarwady delta) (Image Credit: MODIS Rapid Response Project at NASA/GSFC).

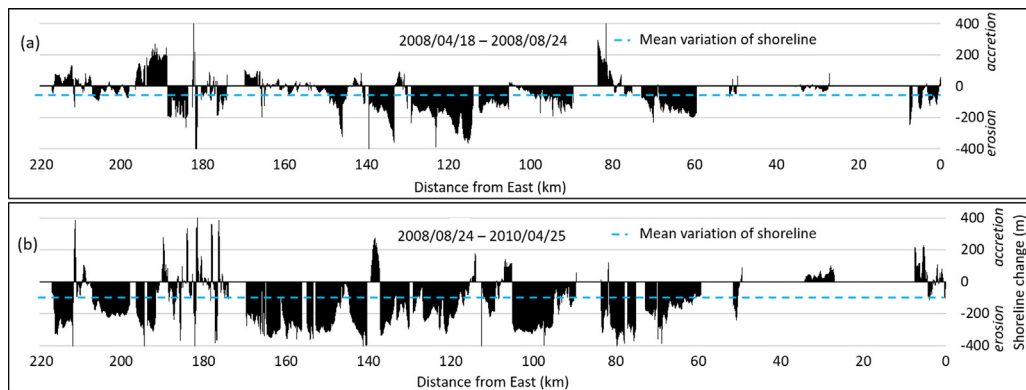


Fig. 5. Shoreline change in the Ayeyarwady delta between 18 April 2008, and 24 August 2008, three months after the passage of cyclone Nargis (a), and between 24 August 2008 and 25 April 2010, 20 months after Nargis (b). The broken line shows the mean shoreline change. See [Fig. 1c](#) for locations of kilometric points alongshore.

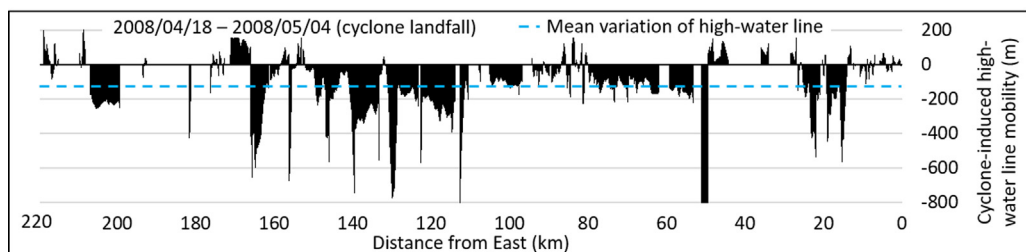


Fig. 6. Position of the high-water line alongshore in the Ayeyarwady delta induced by cyclone surge on 4 May 2008, in the wake of the landfall of Nargis, compared to the high-water line of 18 April 2008. Broken line shows mean high-water line change. The massive landward translation of the high-water line reflects large-scale flooding of the sandy beaches composing the shoreline and of the broad low backshore swales. See [Fig. 1c](#) for locations of kilometric points alongshore.

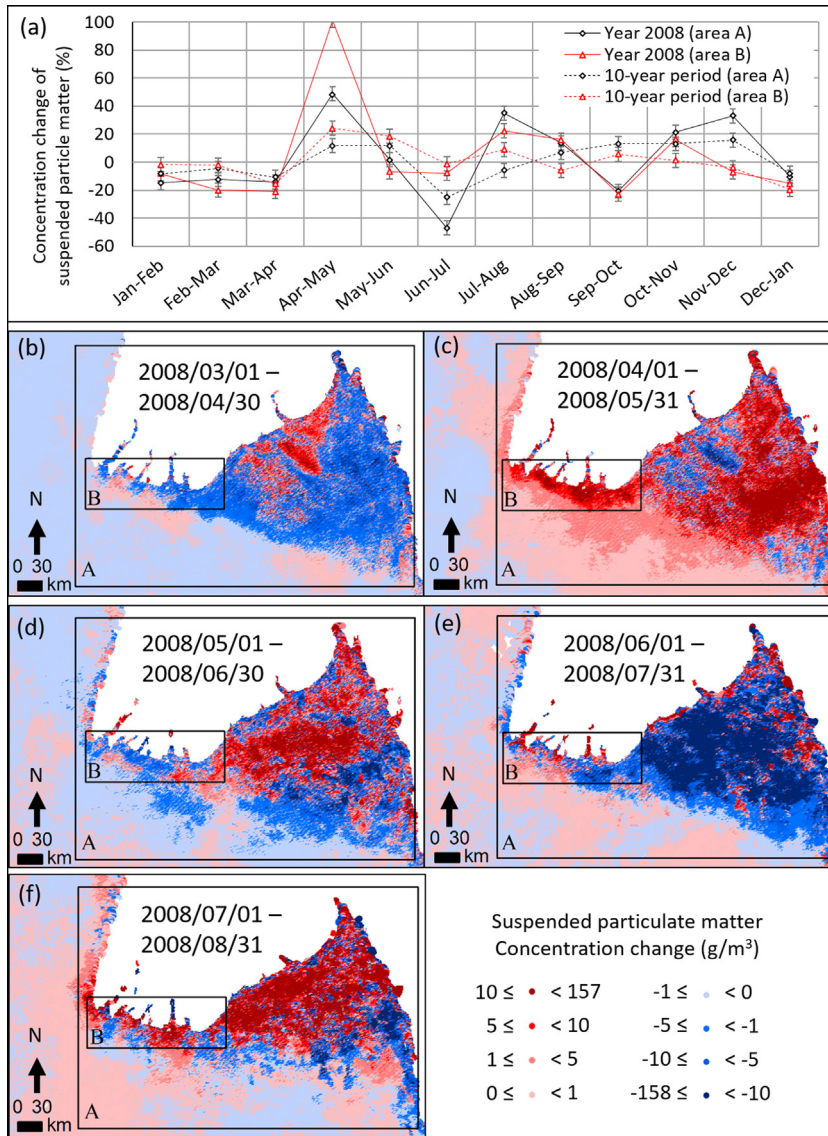


Fig. 7. Suspended particulate matter (SPM) concentrations in the nearshore zone of the Ayeyarwady delta (areas covered are depicted by the rectangles) encompassing the passage of cyclone Nargis (data from GlobCoast project, <http://sextant.ifremer.fr/en/geoportail/sextant>): (a) 2008 values compared to a 10-year average (2002–2012), (b–f) concentration changes over a 2-month time step. Note the following: relatively low dry season concentrations between 1 March and 30 April in the eastern sector dominated by the multiple mouths of the Ayeyarwady, with higher concentrations in the more sheltered sector where mud is stored (b); the strong increase in concentrations in the wake of Nargis between 1 April and 30 May (c); the rapid drop in the western sector between 1 May and 30 June, and the corresponding increase in the sheltered western part of the delta (d), thus suggesting eastward transport of suspended sediments following Nargis; the relatively lower concentrations from 1 June to 30 July, corresponding to the onset of the rainy season (e); and the increase from 1 July to 31 August (f) in response to an increase in river sediment supply during the rainy season.

1974. This suggests that Nargis and other high-energy events that may affect the Ayeyarwady delta in the future may further significantly contribute to delta erosion along the exposed western sector.

The chronic erosion of the western sector of the Ayeyarwady delta shoreline may reflect large-scale adjustments in the supply and distribution of sediments alongshore, with the relatively protected and still prograding muddy sector acting as an active depocentre for suspended sediment transported eastward by waves and currents (Anthony et al., 2017). During the passage of

Cyclone Nargis in May 2008, the SPM concentrations off the Ayeyarwady delta increased considerably, compared to the average monthly conditions over a decade (Fig. 7a, c), and this significant increase can be interpreted as a response to:

- increased fine-grained sediment supply by the river following the heavy rainfall generated by Nargis (Fig. 4a, b);
- reworking of fine sediments at the seaward fringes of the delta by the high waves (Fig. 3b) generated by the cyclone;

- wave- and wind-induced resuspension of fine sediment in the shallow nearshore zone.

Nargis likely led to more significant supply of fluvial mud than under non-cyclone conditions. There is no way of determining, however, the contribution of net fluvial SPM supply to the nearshore zone, compared to remobilization over this muddy zone, although the fact that the month of May merely corresponds to the start of the high-discharge season (when fine-grained fluvial sediment supply is not expected to be at its peak) could be an argument in favour of the exceptional remobilization of shore-front and nearshore mud by the cyclone. The significant drop in nearshore SPM concentrations in June and July (Fig. 7e) is, however, consistent with the overall propensity of the shallow Ayeyarwady delta shoreface to trap muddy sediments, whereas the increase in July and August reflects the seasonal Monsoon river discharge effect. Much of the SPM mobilized by the cyclone moved from west to east across the delta (Fig. 7d), in agreement with the tendency for fine-grained suspension load to be transported towards the more sheltered and embayed eastern sector of the delta (Fig. 1c) in the Gulf of Martaban (Anthony et al., 2017). Presumably, mud was stored within the delta itself and in the immediate shallow nearshore zone, and not lost offshore in this tide- and current-influenced setting, with possibly maximum storage in the relatively sheltered eastern mud depocenter, where the delta is currently prograding.

The vulnerability of the delta is probably mainly the result of reduced sediment supply, further compounded by the impacts of population growth and mangrove deforestation (Brakenridge et al., 2017; Fritz et al., 2009). Modelling of sediment supply based on existing dams on the river's tributaries showed, over a decade ago, an already significant 30% reduction (Syvitski et al., 2005). Discrepancies in the 10-year (2002–2012) GlobCoast data on SPM off the delta preclude confirmation of this drop in the supply of fine-grained sediment, but the reduction highlighted by Syvitski et al. (2005) must be playing a significant role in the sustained coastal erosion. The decrease in sediment load, in the face of relative sea level rise and ongoing subsidence, is also resulting in sinking of the Ayeyarwady delta, generating loss of valuable wetlands, while threatening, over the long-term, the delta's very existence (Syvitski et al., 2009). Various studies have further documented important losses of mangrove forest along the delta to the benefit of shrimp farms and rice cultivation (Frenken, 2012; Giri et al., 2010; Hedley et al., 2010; Leimgruber et al., 2005). According to Hedley et al. (2010), the total mangrove forest area decreased from 2345 km² to 1786 km² between 1924 and 1995 because of clearance for agriculture and aquaculture. It is projected that, if unprotected, the Ayeyarwady delta mangrove forests could be completely lost by 2026 (Webb, 2013), thus depriving the delta shoreline of an important agent in the trapping of fine-grained sediments and especially in coastal protection against cyclones and erosion generated by high Monsoon waves and occasional high-energy events such as Nargis. The Ayeyarwady has been classified, as a result, as a delta "in peril" by Syvitski et al. (2009). This

rising vulnerability goes with a greater exposure of populations and economic activities in the delta to both catastrophic marine and river flooding.

6. Conclusion

The Ayeyarwady River delta is an essentially tide-dominated delta characterized by a coastal morphology of multiple distributary mouths affected by low to moderate energy southwest monsoon waves. Over half of the deltaic shoreline has been undergoing chronic erosion over the last few decades, and the delta is exposed to tropical cyclones that can be devastating, as shown by the example of cyclone Nargis (2–4 May 2008). Assessment of the resilience of the delta to this high-energy event was carried out by analysing before, during, and after Nargis, changes in delta-front SPM concentrations, as well as in the high-water line alongshore used as an indicator of the extent of shoreline flooding by surge in the wake of Nargis, and of net cyclone-generated shoreline retreat months after Nargis. The cyclone resulted in anomalously high nearshore SPM concentrations compared to average concentrations over a 10-year period, followed by an equally rapid drop in concentrations to well below average following this high-energy event. This suggests important temporary resuspension of SPM over the coastal fringes of the delta and the nearshore delta-front, and, possibly, larger-than-usual fine-grained fluvial sediment input to the delta. Nargis resulted in a significant temporary landward translation of the high-water line alongshore, and submergence of the delta's sandy beaches following a high surge level, causing numerous human casualties, and severe socio-economic damage in an increasingly more densely populated delta subjected to large-scale deforestation and mangrove removal. The cyclone also resulted in severe erosion of the shoreline, with no signs of resilience several months after. This vulnerability to erosion was likely aggravated by a condition of decreasing fluvial sediment supply to the delta.

Acknowledgements

We thank WWF Asia for funding of the Project "Recent shoreline changes and morpho-sedimentary dynamics of the Ayeyarwady River delta: assessing the impact of anthropogenic activities on delta shoreline stability" via the Helmsley Foundation. We thank Associate Editors Isabelle Manighetti and Rutger de Wit, and two reviewers, among whom Toru Tamura, for their salient suggestions for improvement of the manuscript. We are especially grateful to Rutger de Wit and an anonymous reviewer for their insightful comments on the analysis of the shoreline data.

Appendix A. Supplementary material

Supplementary material associated with this article can be found in the online version available at <https://doi.org/10.1016/j.crte.2017.09.002>.

References

- Anthony, E.J., 2016. Deltas. Oxford Bibliographies, Geoscience, Oxford University Press (online publication at <http://www.oxfordbibliographies.com/>).
- Anthony, E.J., Besset, M., Dussouillez, P., 2017. Recent Shoreline Changes and Morpho-Sedimentary Dynamics of the Ayeyarwady River delta: Assessing the Impact of Anthropogenic Activities on Delta Shoreline Stability (Unpub. Report). WWF Asia and Helmsley Foundation, Yangon, Myanmar (43 p.).
- Brakenridge, G.R., Syvitski, J.P.M., Niebuhr, E., Overeem, I., Higgins, S.A., Kettner, A.J., Prades, L., 2017. Design with nature: causation and avoidance of catastrophic flooding, Myanmar. *Earth Sci. Rev.* 165, 81–109.
- Bronzizio, E.S., Foufoula-Georgiou, E., Szabo, S., Vogt, N., Sebesvari, Z., Renaud, F.G., Newton, A., Anthony, E.J., Mansur, A.V., Matthews, Z., Hetrick, S., Costa, S.M., Tessler, Z., Tejedor, A., Longjas, A., Dearing, J.A., 2016. Catalyzing action towards the sustainability of deltas. *Curr. Opin. Environ. Sustainabil.* 19, 182–194.
- Coleman, J.M., Huh, O.K., 2004. Major Deltas Of The World: A Perspective From Space. Coastal Studies Institute, Louisiana State University, Baton Rouge, LA, USA (<http://www.geol.lsu.edu/WDD/PUBLICATIONS/C&Hnasa04/C&Hfinal04.htm>).
- Dube, S.K., Murty, T.S., Feyen, J.C., Cabrera, R., Harper, B.A., Bales, J.D., Amer, S. (Eds.), 2010. Storm Surge Modeling and Applications in Coastal Areas. World Scientific Series on Asia-Pacific Weather and Climate Global Perspectives on Tropical Cyclones, Vol. 4, World Scientific Publishing, Singapore, pp. 363–406.
- Ericson, J.P., Vörösmarty, C.J., Dingman, S.L., Ward, L.G., Meybeck, M., 2006. Effective sea level rise and deltas: causes of change and human dimension implications. *Glob. Planet. Change* 50, 63–82.
- Fearnley, S.M., Miner, M.D., Kulp, M., Bohling, K., Penland, S., 2009. Hurricane impact and recovery shoreline change analysis of the Chandeleur Islands, Louisiana, USA: 1855 to 2005. *Geo-Mar. Lett.* 29, 455–466.
- Frenken, K., 2012. Irrigation in Southern and Eastern Asia in figures, AQUASTAT Survey. 2011. FAO Water Reports 37. Food and Agriculture Organization of the UN, Rome487.
- Fritz, H.M., Blount, C., Sokoloski, R., Singleton, J., Fuggle, A., McAdoo, B.G., Moore, A., Grass, C., Tate, B., 2007. Hurricane Katrina storm surge distribution and field observations on the Mississippi Barrier Islands. *Estuar. Coast. Shelf Sci.* 74, 12–20.
- Fritz, H.M., Blount, C.D., Thwin, S., Thu, M.K., Chan, N., 2009. Cyclone Nargis storm surge in Myanmar. *Nat. Geosci.* 2, 448–449.
- Furuichi, T., Win, Z., Wasson, R.J., 2009. Discharge and suspended sediment transport in the Ayeyarwady River, Myanmar: centennial and decadal changes. *Hydrol. Process.* 23, 1631–1641.
- Giri, C., Ochieng, E., Tieszen, L.L., Zhu, Z., Singh, A., Loveland, T., Masek, J., Duke, N., 2010. Status and distribution of mangrove forests of the world using earth observation satellite data. *Glob. Ecol. Biogeogr.* 20, 154–159.
- Hapke, C.J., Reid, D., Richmond, B.M., Ruggiero, P., List, J., 2006. National Assessment of Shoreline Change Part 3: Historical Shoreline Change and Associated Coastal Land Loss Along Sandy Shorelines of the California Coast. USGS Report, Geological Survey, US. 13–14.
- Hedley, P.J., Bird, M.I., Robinson, R.A.J., 2010. Evolution of the Irrawaddy delta region since 1850. *Geogr. J.* 176, 138–149.
- Knapp, K.R., Kruk, M.C., Levinson, D.H., Diamond, H.J., Neumann, C.J., 2010. The International Best Track Archive for Climate Stewardship (IBTrACS): unifying tropical cyclone best track data. *Bull. Am. Meteorol. Soc.* 91, 363–376.
- Kravtsova, V.I., Mikhailov, V.N., Kidyayeva, V.M., 2009. Hydrological regime, morphological features and natural territorial complexes of the Irrawaddy River Delta (Myanmar). *Water Resour. Res.* 36, 259–276.
- Leimgruber, P., Kelly, D.S., Steininger, M.K., Brunner, J., Mueller, T., Songer, M., 2005. Forest cover change patterns in Myanmar (Burma) 1990–2000. *Environ. Conserv.* 32, 356–364.
- Naing, Z., 2014. Ports Development in Myanmar. Oil & Gas conference, Myanmar, 2014. Mandalay Technology. In: http://www.alpha-resources.com/sites/alpha-resources.com/files/download%20file/5.Ports%20Development%20in%20Myanmar_UZawNaing.pdf.
- Ramaswamy, V., Rao, P.S., Rao, K.H., Thwin, S., Rao, N.S., Raiker, V., 2004. Tidal influence on suspended sediment distribution and dispersal in the northern Andaman Sea and Gulf of Martaban. *Mar. Geol.* 208, 33–42.
- Robinson, R.A.J., Bird, M.I., Oo, N.W., Hoey, T.B., Aye, M.M., Higgitt, D.L., Lu, X.X., Swe, A., Tun, T., Win, S.L., 2007. The Irrawaddy river sediment flux to the Indian Ocean: the original nineteenth-century data revisited. *J. Geol.* 115 (6), 629–640.
- Rodolfo, K.S., 1969. Bathymetry and marine geology of the Andaman Basin, and tectonic implications for Southeast Asia. *Geol. Soc. Am. Bull.* 80, 1203–1230.
- Syvitski, J., Vörösmarty, C.J., Kettner, A.J., Green, P., 2005. Impact of humans on the flux of terrestrial sediment to the global coastal ocean. *Science* 308, 376–380.
- Syvitski, J.P.M., Kettner, A.J., Overeem, I., Hutton, E.W.H., Hannon, M.T., Brakenridge, G.R., Day, J., Vorosmarty, C., Saito, Y., Giosan, L., R.J., Nicholls, 2009. Sinking deltas due to human activities. *Nat. Geosci.* 2, 681–686. <http://dx.doi.org/10.1038/ngeo629>.
- Tasnim, K.M., Esteban, M., Shibayama, S., Takagi, H., 2015. Storm surge due to 2008 Cyclone Nargis in Myanmar and post-cyclone preparedness activities. In: Esteban, M., Takagi, H., Shibayama, T. (Eds.), *Handbook of Coastal Disaster Mitigation for Engineers and Planners*. Elsevier Inc., Butterworth-Heinemann, pp. 55–74.
- Topich, W.J., Leitich, K.A., 2013. The History of Myanmar. The Greenwood Histories of The Modern Nations. Greenwood, ABC-CLIO, Santa Barbara, California. (173 p.).
- USAID, 1968. Cyclone, Burma Disaster Relief, May 1968. US Agency for International Development AID, Rangoon, Burma (38 p.).
- Van der Velden, J., 2015. Understanding the Dynamics of the Ayeyarwady River, Myanmar (Master's Thesis). Utrecht University (30 p.).
- Ward, P.J., Jongman, B., Sperna Weiland, F., Bouwman, A., van Beek, R., Bierkens, M.F.P., Ligtoet, W., Winsemius, H.C., 2013. Assessing flood risk at the global scale: model setup, results, and sensitivity. *Environ. Res. Lett.* 8, (10 p.).
- Webb, E.L., 2013. Deforestation in the Ayeyarwady Delta and the conservation implications of an internationally-engaged Myanmar. *Glob. Environ. Change.* 24, 321–333.
- Winsemius, H.C., Van Beek, L.P.H., Jongman, B., Ward, P.J., Bouwman, A., 2013. A framework for global river flood risk assessments. *Hydrol. Earth Syst. Sci.* 17, 1871–1892.
- Wolf, J., 2009. Coastal flooding: impacts of coupled wave–surge–tide models. *Nat. Hazards* 49, 241–260.